Titanium Alloys Manufactured by In Situ Alloying During Laser Powder Bed Fusion

I. Yadroitsev, P. Krakhmalev & I. Yadroitsava

JOM
The Journal of The Minerals, Metals & Materials Society (TMS)

ISSN 1047-4838
Volume 69
Number 12

JOM (2017) 69:2725-2730
DOI 10.1007/s11837-017-2600-7

Springer

JOM, Vol. 69, No. 12, 2017
DOI: 10.1007/s11837-017-2600-7

Titanium Alloys Manufactured by In Situ Alloying During Laser Powder Bed Fusion

I. YADROITSEV,[1,3] P. KRAKHMALEV,[2] and I. YADROITSAVA[1]

1.—Department of Mechanical and Mechatronic Engineering, Central University of Technology, Bloemfontein, Free State 9300, South Africa. 2.—Department of Engineering and Physics, Karlstad University, 651 88 Karlstad, Sweden. 3.—e-mail: iyadroitsau@cut.ac.za

This work is focused on the investigation and understanding of in situ processes in Ti-15%Mo and Ti6Al4V-1.38%Cu alloys by laser powder bed fusion (LPBF). In both materials, Mo and Cu were introduced as elemental powders into the precursor powder mixture. The effect of process parameters, i.e., energy input on surface morphology and homogeneity, was investigated. The importance of different thermophysical properties of blended powders is also discussed. The chemical composition of phases and phase distribution in sintered materials were investigated by means of scanning electron microscopy. The mechanical properties of in situ alloyed as-built LPBF specimens were determined. The results obtained developed knowledge that is important for understanding the in situ alloying process during LPBF, and they create a base for synthesizing new materials.

INTRODUCTION

Laser powder bed fusion (LPBF) is a manufacturing method that can produce objects of complex geometry. As a result, it introduces additional opportunities to synthesize new materials from elemental powders using in situ alloying. The potential of the in situ LPBF alloying approach is nevertheless not well understood because of a lack of experimental knowledge and information on the influence of process parameters on the microstructure, homogeneity, and properties of the final materials.

The benefits of in situ alloying by LPBF to produce new materials with unique properties were shown recently. Vrancken et al.[1] sintered Ti6Al4V-10% Mo alloy to stabilize the β-phase in the LPBF alloy; a combination of excellent ductility and high strength in this alloy was reported. Sistiaga et al.[2] mechanically mixed 4% Si powder (-10 μm) and Al7075 alloy powder with an average particle size of 53 μm and produced dense crack-free parts. Vora et al.[3] demonstrated successful AlSi12 in situ alloy formation from elemental Al (-66 μm) and Si (-100 μm) powders. It was noted that the in situ LPBF alloying method could be potentially cost and time effective in developing new materials.

The materials chosen for this investigation are novel Ti-base materials with enhanced performance. Ti6Al4V is a widely used α-β alloy for biomedical applications; however, its high elastic modulus and low ductility limit its applications for manufacturing direct load-bearing structural implants. Achievements in Ti alloys for biomedical and implant applications resulted in the development of β-Ti alloys that have elastic modulus similar to human bones and alpha-beta alloys with enhanced fatigue properties.[4] Titanium-copper alloys are other novel materials that show particular promise as biomaterial with embedded antibacterial properties, as additions of Cu can decrease bacterial growth at the implant interface.[5–7]

In this research, in situ alloying was achieved by melting a mixture of the precursor powders by LPBF. Materials with vastly different melting points had been chosen. Particle size distribution was similar for all powders (-45 μm). The illustrated effects of process parameters on the properties of the synthesized material are paramount to successful manufacturing of nonporous samples for advanced implants with unique properties. The results obtained developed new knowledge that is important for understanding the in situ alloying process during LPBF and new material production.

(Published online October 6, 2017)

MATERIALS AND METHOD

The experiments were carried out on mixtures of gas-atomized powders of CP Ti (grade 2) with 15 wt.%Mo powder and Ti6Al4V ELI with 1.38 wt.% Cu. Particle size distributions are shown in supplementary Table SI. The mixture of Ti-15%Mo was dried in the oven for about 15 h at a temperature of 85°C, with stirring at 30 min. The mixture of Ti6Al4V-1.38%Cu was dried at 80°C for 2 h. Different procedures for drying were elaborated experimentally because of the very different flowability of the two mixtures.

The experiments were conducted on an EOSINT M280 machine (EOS GmbH) with Argon as the protective atmosphere. The oxygen level in the chamber was less than 0.12%. For single tracks and layers, a uniform powder layer of 60 μm thickness was used. Single tracks were sintered over a wide range of laser powers (50–350 W) and scanning speeds (0.08–3.4 m/s). All tracks were 20 mm in length. For each scanning speed, three single tracks were produced. To investigate the distribution of elements in the bulk material, 3D specimens of 10 × 10 × 5 mm were manufactured at optimal process parameters and hatch distances at 30-μm layer thickness.

RESULTS AND DISCUSSIONS

Conditions for In Situ Alloying

For an in situ alloying process, first, a complete melting of all components in the powder mixture is required. The energy needed for fusion of the unit volume of the material can be estimated with:

$$E = \rho[C \times (T_m - T_0) + L_f], \quad (1)$$

where ρ is the density, C is the specific heat capacity, T_m is the melting point, and L_f is the latent heat of the fusion. If E values for component powders are similar, it means that if the laser provides enough energy input, both materials are molten.

The estimated time of direct interaction of laser beam with powder is

$$t_{D.I.} = d_0/V, \quad (2)$$

where d_0 is the laser beam spot size diameter and V is the scanning speed varied during processing with limitations. Too low laser scanning speeds can result in a transition to a keyhole mode and finally can lead to porous LPBF parts. At a very high laser scanning speed, instability of the track occurs and a balling effect is observed.[8]

During LPBF, sufficient time is required for powder-laser beam interaction and homogenization of the temperature within particles. The temperature homogenization time[9] in powder particles can be calculated as

$$t_{hom} = r^2/a, \quad (3)$$

where r is the powder particle radius and a is the thermal diffusivity of a bulk metal.

In a case of $t_{hom} < t_{D.I.}$, and E is high enough, the powder particles melt. If $t_{hom} \gg t_{D.I.}$, partial melting of the powder material can occur. Complete melting of the powders is a necessary condition for the in situ alloying. Nevertheless, processes in the molten pool, convection, Marangoni flows, density and viscosity gradients, etc., affect in situ alloying. Another two examples are introduced to discuss these conditions based on the experimental observations and investigations of Ti-15%Mo and Ti6Al4V-1.38%Cu alloys manufactured by LPBF in situ.

Ti6Al4V-1.38%Cu Alloy

Analysis of single tracks showed that laser power 170 W and 1.0 m/s scanning speed were optimal for the Ti6Al4V-1.38%Cu powder mixture. An investigation of the homogeneity distribution of Cu in Ti6Al4V on a surface at various scanning speeds near optimum (0.7–1.3 m/s) showed that copper particles melted and created islands following solidification lines (see supplementary Figs. S1 and S2).

Investigations with SEM EDS have shown that Cu dissolved in the Ti alloy, although some areas enriched with Cu were observed. A regular martensitic structure was not pure Ti6Al4V but a material alloyed with Cu. Copper content in these areas varied in the range of 1–1.5 wt.%. This concentration is quite close to the nominal content of Cu powder in the initial powder mixture. In the areas enriched with Cu but still having a martensitic structure, the concentration of Cu varied between 2 wt.% and 5 wt.% (zone 1, Fig. 1b). The highest concentration of Cu, up to 35 wt.%, was observed in areas that have a different microstructure (zone 2, Fig. 1b). Nevertheless, it is possible to conclude that the observed Cu-rich areas were not pure Cu as the concentration of Ti in those areas was high. Furthermore, no unmelted Cu particles were observed in the microstructure.

The inhomogeneity can be explained by taking into account the difference in material properties (Table SI). The energies required for melting the unit volume (Eq. 1) of the bulk Ti6Al4V and Cu are close: 5.67 J/mm^3 and 5.49 J/mm^3, respectively. The estimated time $t_{D.I.}$ of direct interaction of the laser beam and powder under the laser spot size of 80 μm and scanning speed V = 0.7–1.3 m/s, was in the range of 114–61.5 μs. The temperature homogenization time in the solid particles can be calculated accordingly to Eq. 2. For Ti6Al4V, this time is 106 μs, which is about 40 times higher than for Cu (3 μs). This estimation was done for powder particles with a diameter of d_{90} = 37 μm (Table SI). Copper powder particles, therefore, were fused first

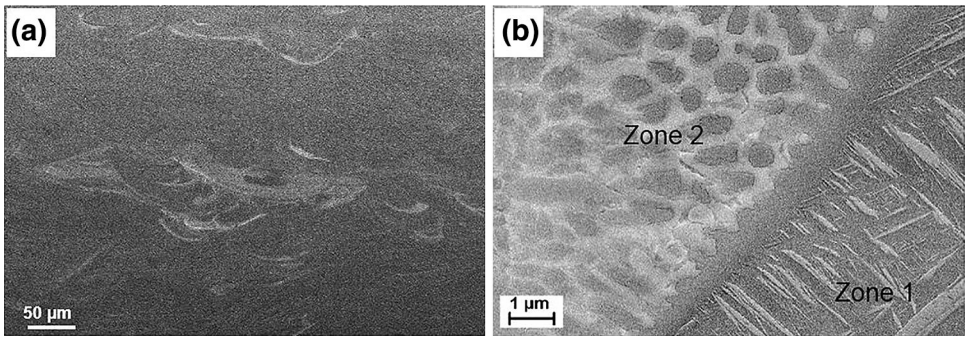

Fig. 1. Copper distribution in Ti6Al4V ELI matrix at different magnifications: total view (a) and area enriched with Cu (b).

and transferred heat quickly to the surrounding titanium alloy. In principle, the conditions for in situ alloying were satisfied and both powders were completely molten under the indicated process parameters.

The viscosity of liquid Ti at temperatures of 1750–2050 K is 4.42 mPa × s.[10] For pure liquid copper, the viscosity changes from 4.03 mPa × s at 1356 K to 1.96 mPa × s at 1950 K.[11] Drops of liquid copper with low viscosity were distributed in a viscous liquid titanium alloy during LPBF. As a result of short interaction times, there was insufficient mixing for complete homogenization, and the Cu-rich regions solidified in the matrix of the Ti6Al4V. Density is another factor influencing inhomogeneity of the in situ alloying. Liquid Cu has a higher density and sinks to the bottom of the molten pool with agglomeration near the fusion boundaries. Therefore, although the necessary conditions for in situ alloying were satisfied and both materials were completely molten, the differences in density and viscosity resulted in inhomogeneity and formation of Cu-rich regions at the periphery of the molten pool (Figs. 1, S1, and S2). Possibly, a new set of manufacturing parameters, guaranteeing more intensive flows and longer times of existence of the liquid phase, has to be developed to manufacture a more homogeneous Ti6Al4V-1.38%Cu alloy.

Ti-15%Mo Alloy

The range of scanning speeds for producing continuous single tracks generally increased with laser power for in situ sintered Ti-15%Mo (Fig. S3). At a higher laser power, the temperature of the melt pool increased, which improved wetting conditions for the molten powder.[12,13] The remelted depth increased at low scanning speeds, which created an additional stabilizing effect on single tracks and expanded the zone for continuous tracks.[8]

The shape of the single tracks formed at laser powers of 100 W, 150 W, 200 W, 300 W, and 350 W and their corresponding scanning speeds of 0.4–0.5 m/s, 0.6–1.2 m/s, 1.0–1.2 m/s, 1.8–2.2 m/s, and 2.4–2.8 m/s respectively, closely resemble a semicircular shape. Such a mode leads to good bonding between the tracks and the substrate, and could be referred to as the optimum set of process parameters. At laser powers of 300 W and 350 W and scanning speeds in the range of 1.2–1.6 m/s and 1.2–2.0 m/s, respectively, the penetration depth exceeded the height and width of the tracks 1.5–2 times. The excessive laser energy per unit volume caused a keyhole mode of laser melting.

An SEM EDS analysis showed that Mo was randomly distributed in the Ti matrix (Fig. 2). The microstructure consisted of a portion of lamellar structure, areas with cellular dendritic structure, and unmolten particles of Mo. Boundaries of vertical colonies were visible in the optical microscope. Irregular grain boundaries also were found by SEM in cross sections of 3D samples perpendicular to the building direction (Fig. 2). Martis et al.[14] described a similar structure in Ti-15%Mo after hot swaging. It was suggested that when fast cooling took place, the structure did not have sufficient time to form a more stable configuration, so the microstructure had irregular grain boundaries.

The LPBF structure consisted of regions of α-hexagonal phase commonly forming a lamellar structure and regions of the β-cubic phase formed a cellular dendritic structure that formed during solidification (Fig. S4). The alloy was not homogeneous: the average concentration of Mo in the alloy was 7.5–15 wt.%. Concentrations of Mo observed in the alloy correspond well to the bimodal $\alpha + \beta$ microstructures. Ho et al.[15] indicated that for Ti-x%Mo alloys, when the Mo content increased to 10 wt.% or higher, the retained β-phase became the dominant phase.

The energy required for melting of a unit volume of solid Ti and Mo, estimated with Eq. 1, was 5.82 J/mm^3 and 8.74 J/mm^3, respectively. Thus, the energy input needs to be about 1.5 times higher to melt a similar volume of Mo compared with that of Ti. Numerical simulations executed as described in Ref. 16 showed that the penetration depth for pure Mo was 11 μm at 150-W laser power and 1.0-m/s scanning speed. At similar P and V, the Ti molten

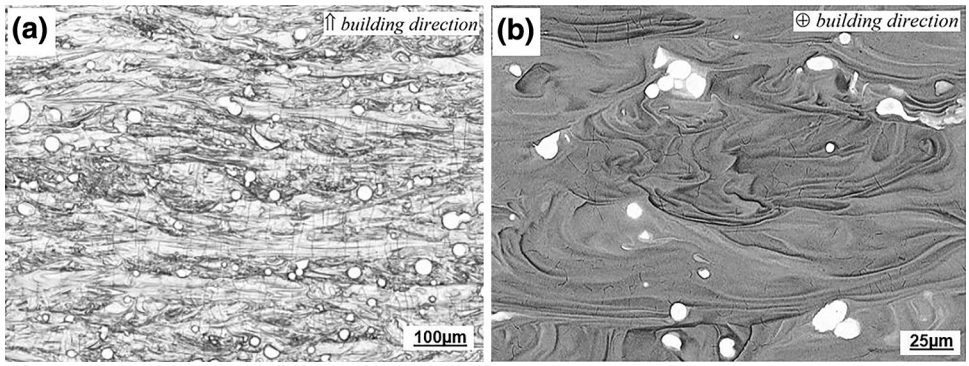

Fig. 2. Microstructure of LPBF Ti-15%Mo samples at 150-W laser power, 1.0-m/s scanning speed, and 80-μm hatch distance: image from optical microscope (a) and by SEM in BSE mode (b).

pool had an elongated shape with 52-μm maximal depth and 210-μm length (Fig. S5). Although simulations were done for bulk materials and disregarded actual interaction of the laser beam powder, it fits experimental observations quite well. SEM assessment of unmolten Mo particles in the Ti-15%Mo alloy showed that all those particles were about 15–20 μm in size or larger. Thus, the input energy was sufficiently high to melt Ti particles completely but not all the Mo powder, as a result of the thermophysical property differences between the two materials. The laser radiation reflectance of Mo is higher than that of Ti;[17] hence, Ti powder would absorb more laser radiation than Mo. These factors lead to the complete melting of Ti and to the partial melting of Mo at the selected manufacturing conditions and powder size distribution.

The estimated time of direct interaction of the laser beam with the surface of the solid material under a laser spot size of 80 μm and scanning speed V = 1.0 m/s was 80 μs (Eq. 2). This was enough time for temperature homogenization in both the Ti and Mo powders. Mo particles of 25 μm in diameter become uniformly heated after about 2.5 μs, while Ti particles with similar diameter needed 22 μs for temperature homogenization (Eq. 3). Another factor influencing the inhomogeneity that was observed is the behaviour of particles in the molten pool. The viscosity of liquid Ti at temperatures of 1750–2050 K is 4.42 mPa $\times$ s, and for liquid Mo, the viscosity is 5.39 mPa $\times$ s.[10,18] Since the viscosity is quite similar, it seems that the mixing in the liquid phase in the To-Mo alloys was better compared with that in the Ti6Al4V-xCu alloy. Fine Mo particles that were molten mixed better in the base material, but the coarser fraction of Mo particles were not completely molten. Unmolten and heavy Mo particles sink down to the bottom of the molten pool transferring their heat quickly to the surrounding alloy. Rather sharp borders between big partially melted Mo particles and the surrounding Ti-Mo alloy were found (Fig. 2b). The Ti molten pool existed for about 250 μs, whereas for Mo, this value was about three times lower (Fig. S5).

The absence of a broad gradient zone between particles and the surroundings confirms that there was not sufficient diffusion, most probably as a result of a drop in temperature. The main reason for inhomogeneity in the investigated Ti-Mo alloy, therefore, was incomplete melting of the coarse fraction of Mo particles. To achieve homogeneous distribution of elements, selection of Mo powder with different particle size distributions, with coarse particles not exceeding 11 μm in size, is recommended for the selected process parameters.

Mechanical Properties of In Situ Alloyed Samples

The Vickers hardness of the LPBF Ti6Al4V-1.38%Cu was higher than in as-built Ti6Al4V ELI samples (Table I). Ultimate tensile strength (UTS) for the as-built Ti6Al4V (ELI) mini-samples was 1243 $\pm$ 49 MPa,[19] whereas in situ alloying with Cu led to the substantial increase in UTS, up to 1550 $\pm$ 126 MPa.

Cu is known as a β-stabilizer in titanium alloys. Therefore, it is possible that in the areas with a higher Cu concentration, an intermetallic Ti_2Cu or Ti β-phase was formed. Guo et al.[22] have found the presence of hard intermetallic compounds in LPBF Ti6Al4V-x%Cu alloys after water quenching. A relative diffraction intensity of the Ti_2Cu phase gradually increased with the Cu contents. It was suggested that the intermetallic phase in Ti6Al4V-x%Cu alloys could result in higher values of hardness and UTS and, at the same time, some embrittlement of in situ alloyed samples.[22] The solid solution strengthening effect of Cu in titanium alloy and the refinement of martensitic lamella are the other possible factors influencing the enhancement observed in hardness and UTS in the Ti6Al4V-1.38%Cu alloy under investigation. Nevertheless, the mechanisms behind the strengthening effect of Cu in in situ alloyed Ti6Al4V-xCu have to be investigated more thoroughly and be proven by experimental investigations and phase identifications in sintered LPBF material.

Table I. Mechanical properties of Ti alloys

Material	Vickers hardness	Ultimate tensile strength, MPa	Elongation, %
LPBF Ti6Al4V ELI[a]	389 ± 14.8[20]	1243 ± 49[19]	6.6 ± 0.4[19]
LPBF Ti6Al4V-1.38%Cu[a]	456 ± 20	1550 ± 126	4.53 ± 1.60
LPBF Ti-15%Mo[a]	435 ± 35	894 ± 24	2.82 ± 1.77
Cast Ti-15%Mo[21]	310 ± 10	921 ± 19	25 ± 2
Cast Ti6Al4V[21]	294 ± 6	1173 ± 17	6 ± 1

[a]Measured in mini-samples.

Elongation at break also was influenced by alloying. In Ti6Al4V (ELI) mini-samples, elongation at break was more stable and had an average value of 6.6 ± 0.4%.[19] In the as-built Ti6Al4V-1.38%Cu and Ti-15%Mo specimens, experimentally observed elongation to break varied noticeably. Deviation of ductility characteristics is not unusual for additive manufactured materials, especially in mini-samples, and besides the properties of the material itself, they are often related to manufacturing defects and porosity. In the present study, inhomogeneity of alloys influenced the mechanical properties of the mini-samples.

In situ alloyed LPBF Ti-15%Mo had higher Vickers hardness and lower tensile strength than Ti6Al4V (Table I), which was similar to as-cast alloys. Ho[15] supposed that as-cast β-phase alloys had a higher hardness level than α' alloys probably as a result of a stronger solid solution effect. It was found that the hardness in alloys with 6–20% of Mo had a complex dependence on the Mo content, and it was suggested that solid solution strengthening, precipitation hardening, strain-aging, grain size, and phases (α', α'' and β) could affect the hardness of the Ti–xMo alloy. For cast Ti-15%Mo alloy, values of 300–330 HV were indicated.[15,23] In the present study, high hardness and low ductility in as-built LPBF material, in comparison with alloys made by the conventional method, is connected to different thermal history and higher temperature gradients in the LPBF process.

CONCLUSION

In situ alloying was found to be an efficient way to manufacture new materials by LPBF; nevertheless, to manufacture a homogeneous alloy is a challenge. For efficient in situ LPBF alloying processes, not only laser power, scanning speed, and hatch distance should be optimized. An analysis of material properties and powder size has to be done to guarantee efficient melting and intermixing of both materials.

Tensile mini-samples were effective for the determination of the properties of homogenous LPBF material. For in situ alloying by LPBF, mechanical properties also have to be verified with standard samples. The higher hardness observed is quite typical for materials manufactured by LPBF and is the explanation for the fine microstructure and inhomogeneity formed in the in situ alloys under investigation. The influence of the manufacturing method on the ultimate tensile strength is different. The UTS can increase as a result of alloying or precipitations effects, as was observed in the Ti6Al4V-1.38%Cu material, or decrease as a result of the influence of unmolten Mo particles in the Ti-15%Mo alloy. Elongation of LPBF materials is commonly quite low, which in this case is a result of the inhomogeneous multiphase microstructure of the in situ alloys.

In the present investigations, the size of the Mo powder was too large, and therefore incomplete melting of Mo powder particles was observed. Future research should consider optimal Mo particle sizes to enhance the homogeneity of in situ alloyed Ti-15%Mo and its influence on mechanical properties. In LPBF Ti6Al4V-1.38%Cu material, some inhomogeneity was also observed. Areas of enhanced Cu concentrations were associated with fusion boundaries. Enrichment with Cu differed from area to area. Differences in density and viscosity of molten material were discussed as origins of this type of inhomogeneity.

ACKNOWLEDGEMENTS

This work is based on research supported by the South African Research Chairs Initiative of the Department of Science and Technology and the National Research Foundation of South Africa (Grant 97994) and the Collaborative Program in Additive Manufacturing (Contract CSIR-NLC-CPAM-15-MOA-CUT-01).

ELECTRONIC SUPPLEMENTARY MATERIAL

The online version of this article (doi:10.1007/s11837-017-2600-7) contains supplementary material, which is available to authorized users.

REFERENCES

1. B. Vrancken, L. Thijs, J.-P. Kruth, and J. Van Humbeeck, *Acta Mater.* 68, 150 (2014).
2. M.L.M. Sistiaga, R. Mertens, B. Vrancken, X. Wang, B. Van Hooreweder, J.-P. Kruth, and J. Van Humbeeck, *J. Mater. Process. Technol.* 238, 437 (2016).
3. P. Vora, K. Mumtaz, I. Todd, and N. Hopkinson, *Addit. Manuf.* 7, 12 (2015).
4. J.A. Disegi, M.D. Roach, R.D. McMillan, and B.T. Shultz-abarger, *J. Biomed. Mater. Res. B* 105, 2010 (2016).
5. T. Shirai, H. Tsuchiya, T. Shimizu, K. Ohtani, Y. Zen, and K. Tomita, *J. Biomed. Mater. Res. B* 91, 373 (2009).
6. C. Jung, L. Straumann, A. Kessler, U. Pieles, and M. de Wild, *BioNanoMat*. 15, S180 (2014).
7. A. Kinnear, T.C. Dzogbewu, I. Yadroitsava, and I. Yadroitsev, in *Proceedings of 17th International Conference RAPDASA*, Pretoria, South Africa, Nov 2016.
8. I. Yadroitsev, A. Gusarov, I. Yadroitsava, and I. Smurov, *J. Mater. Process. Technol.* 210, 1624 (2010).
9. P. Fischer, V. Romano, H.P. Weber, N.P. Karapatis, E. Boillat, and R. Glardon, *Acta Mater.* 51, 1651 (2003).
10. P.F. Paradis, T. Ishikawa, and S. Yoda, *Int. J. Thermophys.* 23, 825 (2002).
11. M.J. Assael, A.E. Kalyva, K.D. Antoniadis, R.M. Banish, I. Egry, J. Wu, E. Kaschnitz, and W.A. Wakeham, *J. Phys. Chem. Ref. Data* 39, 033105:1 (2010).
12. I. Yadroitsev, P. Bertrand, and I. Smurov, *Appl. Surf. Sci.* 253, 8064 (2007).
13. D. Wang, Ch. Yu, X. Zhou, J. Ma, W. Liu, and Z. Shen, *Appl. Sci.* 7, 430 (2017).
14. J.R.S. Martins Júnior, R.A. Nogueira, R.O. de Araújo, T.A.G. Donato, V.E. Arana-Chavez, A.P.R.A. Claro, J.C.S. Moraes, M.A.R. Buzalaf, and C.R. Grandini, *Mater. Res.* 14, 107 (2011).
15. W.F. Ho, C.P. Ju, and J.H. Lin, *Biomaterials* 20, 2115 (1999).
16. I. Yadroitsev, P. Krakhmalev, and I. Yadroitsava, *Addit. Manuf.* 7, 45 (2015).
17. E. Palik, eds., *Handbook of Optical Constants of Solids*, 1st ed. (Waltham: Academic Press, 1998), p. 999.
18. T. Iida and R.I.L. Guthrie, *The Thermophysical Properties of Metallic Liquids, Vol. 2, Predictive Models*, 1st ed. (New York: Oxford University Press, 2015), pp. 460–461.
19. I. Van Zyl, M. Moletsane, P. Krakhmalev, I. Yadroitsava, and I. Yadroitsev, *S. Afr. J. Ind. Eng.* 27, 192 (2016).
20. M.G. Moletsane, P. Krakhmalev, N. Kazantseva, A. du Plessis, I. Yadroitsava, and I. Yadroitsev, *S. Afr. J. Ind. Eng.* 27, 110 (2016).
21. W.F. Ho, *J. Alloys Compd.* 464, 580 (2008).
22. S. Guo, Y. Lu, S. Wu, L. Liu, M. He, C. Zhao, Y. Gan, J. Lin, J. Luo, X. Xu, and J. Lin, *Mater. Sci. Eng. C* 72, 631 (2017).
23. J.R.S. Martins Jr., R.O. Araújo, T.A.G. Donato, V.E. Arana-Chavez, M.A.R. Buzalaf, and C.R. Grandini, *Materials* 7, 232 (2014).